11TH INTERNATIONAL SYMPOSIUM ON PARTICLE IMAGE VELOCIMETRY – PIV15
Santa Barbara, California, September 14-16, 2015

Volumetric 3D PIV in heart valve flow

Franziska Hegner[1], David Hess[2] and Christoph Brücker[1]

[1] Institute of Mechanics and Fluid Dynamics, University of Freiberg, Germany
Franziska.Hegner@imfd.tu-freiberg.de

[2] Dantec Dynamics A/S, Skovlunde, Germany

ABSTRACT

The pulsating flow through a mechanical three leaflet heart-valve using 3D PTV and 3D PIV methods was studied. An artificial heart valve and a transparent silicone model, which were already in usage for 3D Scanning Stereo PIV measurements, were mounted in a fluid tank. Three high speed cameras were arranged around the hexagonal basin recording the particle movement in a laser illuminated volume including the heart valve and the first two thirds of the aortic root. A typical stroke volume flow rate for juvenile of 35 ml per beat was pumped through the arch, representing the opening and closing of the heart valve within a cycle of 300 ms. At the beginning of the heart cycle a wash-out flow was generated. During the second phase of the systole, the velocity and the core diameter of the flow diminished and retrograde flow occurred. Regions of particles with long residence time in the arch started to grow, when first separation took place. As well a few counterclockwise traces with a helical like structure could be seen. At the end of the cycle, the flow contained multiple, small-scale eddies and counter eddies whose distribution and movements are now chaotic.

1. INTRODUCTION

The aorta being largest and most proximal artery to left-ventricle is the most important artery in cardiovascular systems. Because of different reasons, the blood flow inside the aorta is a highly non-uniform phenomenon. Firstly the pulsating inflow coming from left ventricle, secondly the curvature of the aortic arch, thirdly tapering descending aorta and at last arteries branching form the main aorta [1]. Due to potential application to diagnosis and prevention of cardiovascular diseases, e.g. atherosclerosis, flow studies through the human aorta play a key role in different research fields. Artificial heart valves can damage blood, generate stenosis [2] and induce inhomogeneous flow profiles, that differ markedly from the flow pattern of a native valve, which is homogeneous and nearly circular [3]. The inhomogeneous flow profiles are characterized by the coexistence of zones with high flow rate and stagnation areas [4]. Due to the high velocity gradients between these two boundaries, high shear stress and turbulences are formed, which can cause sublethal or lethal damage at the cellular blood components as well as in the endothelial cells of the aorta [5].

To optimize and to compare the available valves, three-dimensional flow field data, experimental and numerical, are necessary. In this study 3D PTV and 3D PIV were used methods, which allowed accurate reconstruction of single particle trajectories over a long observation time. This enables studying single particle trajectories and global velocity fields. The pulsating flow (flow rate of 35 ml/beat) through a mechanical three leaflet heart-valve was driven by a linear actuator. Three dimensional three component measurements were carried out in an illuminated volume using three high-speed cameras. Data analysis show complex flow structures through the aortic arch in a 3D volume for a better understanding of the interaction of the heart valve, the flow and the inner walls. The results show the complexity of the pulsating flow that is generated in the aortic arch and allow further to reconstruct the residence time of particles and shear load within different areas of the aortic arch.

2. MATERIAL AND METHODS

2.1. MODEL

The transparent aortic arch model was casted out of silicon (Elastosil RT 601™, refractive index $n \approx 1.4095$). It was already used for earlier 3D Scanning Stereo PIV measurements, see Hegner et al. [6] for more information about the manufacturing of the model. In the following table the main dimensions of the artic geometry referring to Fig. 1 are shown. The diameter of the aorta with 25 mm was adapted to the diameter of the used mechanical heart valve. As mentioned in [6] the non-dimensional physical parameter of the flow represented by the Reynolds- and the Strouhal-number were preserved in the experimental study and agreed with those for blood flow in juvenile heart valves. The natural flow situation was ensured by using a water-glycerin mixture for the larger sized model. For the flow in the larger vessels of the circulatory system, the non-Newtonian behavior of blood was negligible.

Tab. 1 Main dimensions of the aortic geometry by Vasava et al. [1] under normal pressure conditions (80-120 mmHg)

Artery properties	Dimension (mm)
Ascending and descending aorta lumen diameter	25
Brachiocephalic artery (BA) lumen diameter	8.8
Left common carotid artery (LCA) lumen diameter	8.5
Left subclavian artery (LSA) lumen diameter	9.9
Diameter of the bulbs	21

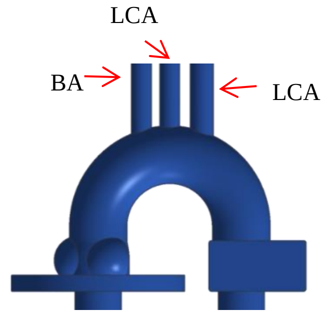

Fig. 1 CAD - Model of the aortic model including the cerebral vessels.

2.2. EXPERIMENTAL SET-UP

The experiments were carried out in a transparent glass tank (width/depth: 190 mm, height: 500 mm) using a glycerin-water solution (58/42 % by mass) as working fluid to ensure refractive index matching with the transparent aortic model. A high-speed pulsed Nd:YLF-Laser (Litron Lasers, Rugby, England, 30 mJ @1,1.3 kHz) was used and illuminated a volume of approximately 70 x 70 x 30 mm³. Three high-speed cameras Cam#1, Cam#2 and Cam#3 (Phantom 12.1, Vision Research, Wayne, New Jersey, resolution at 1280 × 800 pix²) were arrange around the glass tanks, recording simultaneously the particle flow (see Fig. 2). Two cameras were arranged at an angle of 45° and one camera in viewing direction normal to the illuminated volume. All cameras were synchronized with the pulse-laser running at 1000-1300 fps. 60 µm polyamide (PSP) particles which where coated with rhodamine dye (Vestosint, Evonik Degussa GmbH, Essen, Germany, mean diameter 60 µm) were used. To block out reflections on the surface of the silicon model and only recording the coated particles, 60 mm macro lenses with a color filter of 550 nm were mounted on each camera. Scheimpflug adapters were used to tilt the focal plane and secure a focused field of view at lower f-numbers. Directly on top of a mechanical heart valve (three leaflet heart-valve, Triflo trileaflet) the silicone model of the aortic arch was placed. A linear actuator (MOOG, AC-Servo-Actuator, Böblingen, Germany) generated a typical pulsating flow, with a profile as shown in Fig. 3 to represent the systolic phase of the heart cycle. This leads to a stroke-volume with a physiological value of 35 ml/beat, which is a typical stroke volume for children as described by Sproul and Simpson [7].

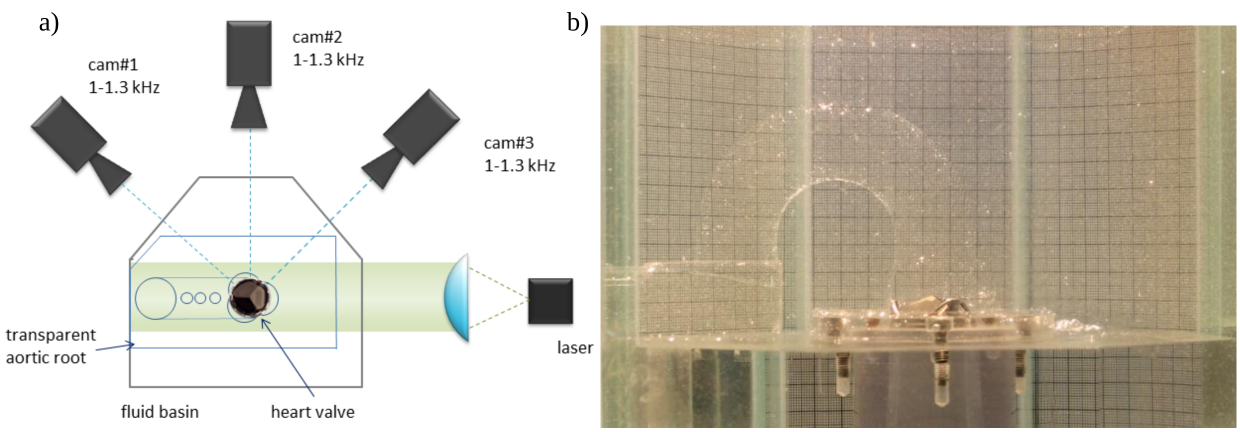

Fig. 2a) Schematic top view of the experimental set-up: the laser illuminated the volume inside the aortic arch, while three high speed cameras recorded the individual particle movement at 1 or 1.3 kHz. The glass tank was filled with a water-glycerin solution to ensure a refractive index matching between the transparent aortic model and the fluid. b) Refractive index matching of the transparent silicon model (Elastosil RT 601™).

To represent the typical diastolic heart pressure of 80 mmHg (= 10.7 kPa) a glycerin-water level of 170 mm over the heart valve was applied. In table 2, the used experimental parameters can be found. Due to the higher viscosity of the fluid, the peak Reynolds-number was in the range of 2691 which hold for juveniles with a lower stroke volume. The post processing of all experimental results was performed in DynamicStudio 2015a (Dantec dynamics, Tonsbaaken, Denmark) and Tecplot 360 2013R1 (Tecplot Inc. Bellevue, Washington, USA).

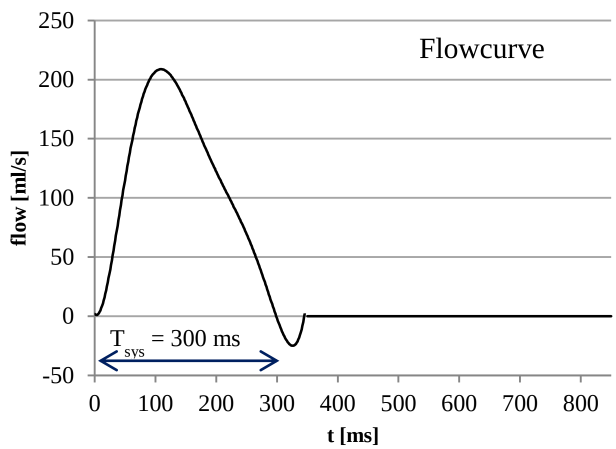

Fig. 3 Systolic flow cycle profile for one cycle of duration T = 850 ms, see e.g. Brücker et al. [2]. 35 ml per beat were pumped during opening and closing of the heart valve within a cycle of T_{sys} = 300 ms.

Tab. 2 Experimental parameters and dimensions

Parameters	Dimension
Density of water-glycerin solution	1.1483 kg/m³
Dynamic viscosity	9.6 mPa s
Refractive index silicone	1.4095
Flow rate per beat	35 ml
Measure volume	70 x 70 x 30 mm³
Frame rate	1000 - 1300 fps
Overpressure	87 mbar
Reynolds-number	2691

3. RESULTS

3.1. 3D PTV

3D PTV and Tomo PTV methods are used to obtain Lagrangian flow fields from the measurements. Tracer particles in the illuminated volume were captured by the multi camera system and analyzed with DynamicStudio 2015a, resulting in single particle trajectories over a long observation time as shown in Fig 4. The Lagrangian trajectories of the particles through the aortic arch were captured during a complete cycle of the heart valve (see Fig. 4a). A complex 3D flow was found, in dependence of the different states of the generated flow. For a better overview, the heart cycle was divided into three periods. The first period ranges from 0-100 frames (≙ 0-100 ms), the 2nd from 100 to 200 frames (≙ 100-200 ms) and the 3rd from 200 – 347 frames (≙ 200 – 347 ms).

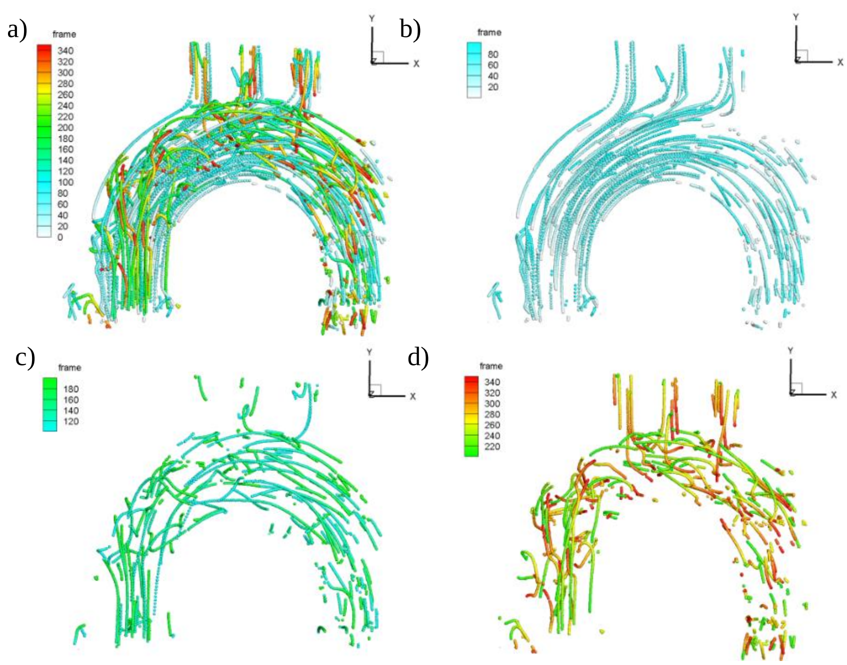

Fig. 4: View on the particle tracks. a) Complete heart valve cycle. b) 1st period (0-100 frames). c) 2nd period (100 – 200 frames). d) 3rd period (200 – 347 frames). The colorbar presents the different frames.

At the beginning of the cycle (1st period), a wash-out flow was generated, which could be seen in linear and homogenous particle traces (see as well Fig. 5, first column). As well a strong washout through the cerebral vessels was observed. The residence time of the particles was low due to the high velocities in the beginning of the heart valve cycle (see chapter 3.2). For the 2nd period, flow separation started to took place and first retrograde traces of the particles, meaning the particle movements running counter to the main forward stream, could be seen. Backflow regions developed near the inner and outer wall and inside the vessels. Within these areas, the residence time of the particles started to grow. Due to the inertia of the flow, the outer regions close to the wall reacted first to the reversal of the pressure gradient. As well a few counterclockwise traces with a helical like structure were seen, with a rotation like that of a corkscrew which is clockwise when viewed in the direction of forward movement [10]. At the end of the systole cycle (3st period), backflow particle traces developed in the ascending and descending arch. Lower velocities were found due to shorter particle trails, which seemed more chaotic and recirculation region spread over the complete area.

3.2. 3D PIV

By using the 3D PIV method the global velocity field was obtained by using a particle density of up to 0,027 per pixel. Voxel volumes were reconstructed using a SMART approach (see [8]) and a 3D LSM algorithm [9] was used, resulting in an Eulerian 3-D velocity field with a volume of 70 x 70 x 30 mm³. Due to the measurement set-up restriction it was only possible to analyze the ascending and distal aortic arch. The first column in Fig. 5 shows multi-exposed pictures of the particle movement in the middle layer taken from earlier measurements with the scanning PIV (see [6]). Multi-exposed pictures of the volumetric measurements would be lead to a losing on information about what happened in the middle layer, due to particles masking them out. The heart cycle phase is displayed in the systole diagram by a green dot. Column two to four showing the velocity field analyzed with DynamicStudio and visualized with Tecplot. The XY-plane of the middle layer is shown in columns two. Column three presents an isometric view of the velocity field and iso-surfaces for different velocities values. In the last column the velocity field in XZ-plane can be found, the position of this plane is illustrated in the first picture of column one by a red line. All velocity fields are in the same order of time as the multi-exposed pictures.
In the beginning of the systolic cycle, the heart valve begins to open and a wash-out flow through the whole aortic arch including the bulbs is generated. This is seen in a homogeneous fluid transport along the arch with velocities at the walls of 0.2 to 0.4 m/s (see first row and particle traces in Fig. 4). In this acceleration phase no flow separations occur and the main flow core is shifted towards the inner wall (wall with lower radius of curvature). The peak velocities of 0.9 m/s can be found for the time steps T = 80 ms (second row) and the core is slightly shifted to the outer wall, seen in the XZ-plane. In late systole (row three to five) the core flow shrinks in diameter and declines while retrograde flow regions develop close to the outer contour of the arch with relatively low velocities. At the inner curvature separation of the flow started as well.

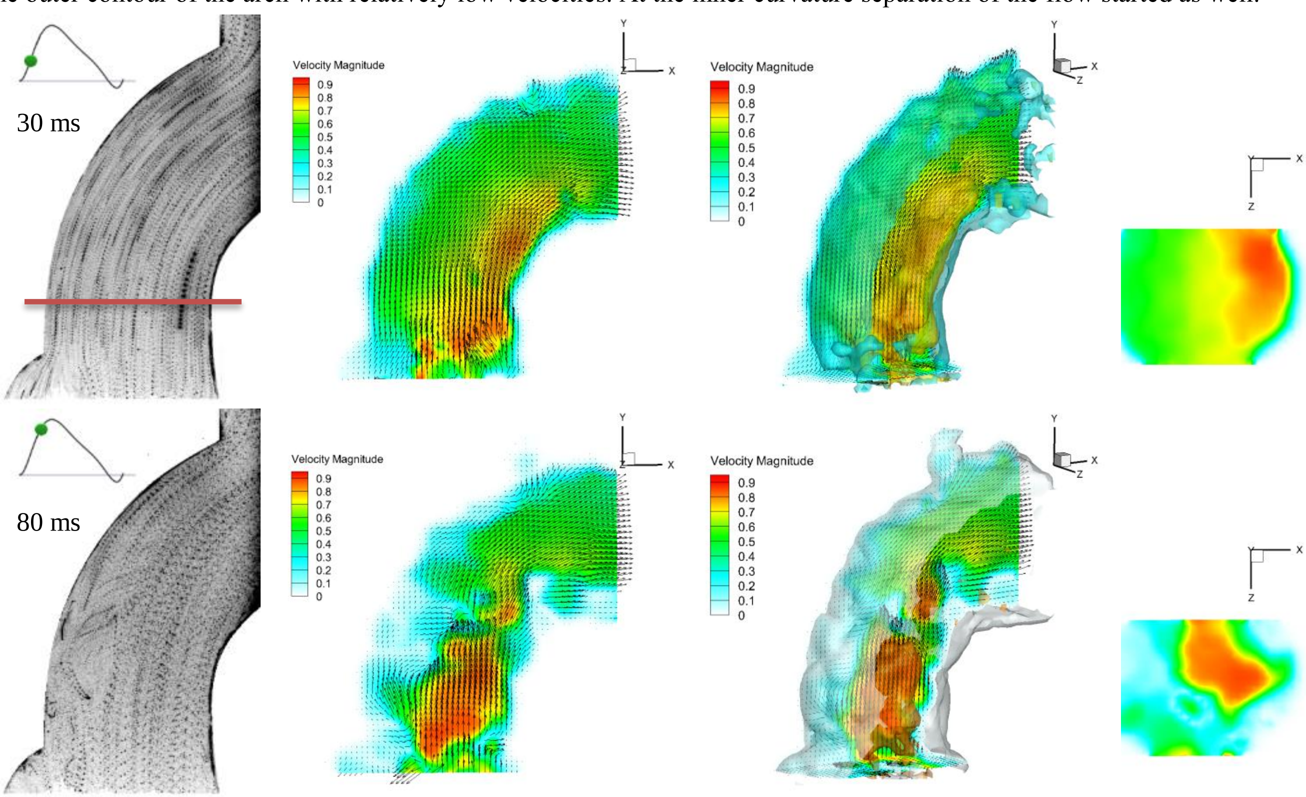

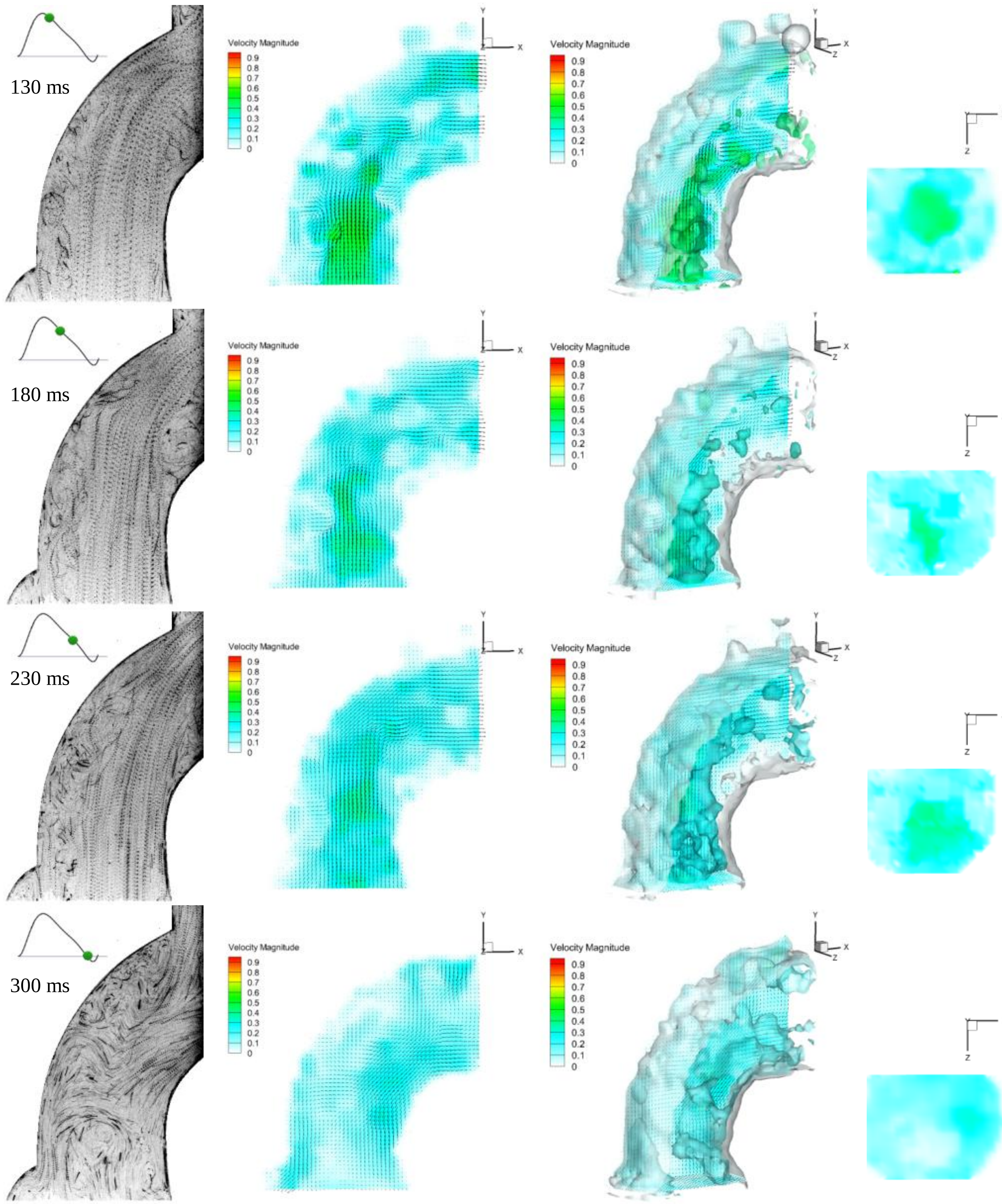

Fig. 5: Visualizations of the particle movement and the velocity fields at six different phases of the systole cycle. First column shows multi exposure picture of particle displacement for one light-sheet (LS) from earlier measurements [see 6]. The LS is aligned in the middle of the aortic arch. Column two to four showing the analyzed velocity field, the XY-plane, an isometric-view with different iso-surfaces and the XZ-plane.

At the end of the cycle at 300 ms the flow contains multiple, small-scale eddies and counter eddies whose distribution and movements are now chaotic. High shear stress values are expected in regions where high velocity gradients are found. Retrograde flow developing on the walls, shear against the main core flow and increases the tangential stress.

In the following Fig. 6 the iso-surface velocity distribution for 6 different times after the opening of the heart valve are presented. All velocities ranging over 0.1 m/s are cut off and the iso-surfaces are grouped into three velocities to represent the velocity fields near the walls. Blue is 0.01 m/s, green 0.05 m/s and red stands for a velocity of 0.1 m/s. Shortly after the opening of the valve, the velocities in the whole arch range over 0.1 m/s. Only in the right part of the bulbs the velocity is under 0.1 m/s. At 80 ms, the velocity starts to be low at the outer wall, this also can be found for some spots at the inner curvature. For a time step of 130 ms the shear layer rolls up, in a wave like structure at the outer wall. This happened with a certain frequency seen in four streams similar to a rip (shown by four arrows pointing on them). With growing time the velocity is decreased in the outer/inner wall regions, as well as in the cerebral vessels. At 180 ms the velocity in the middle of the lower arch is decelerated to the end of the heart cycle (300 ms), where low velocity regions starts to spread over the complete arch.

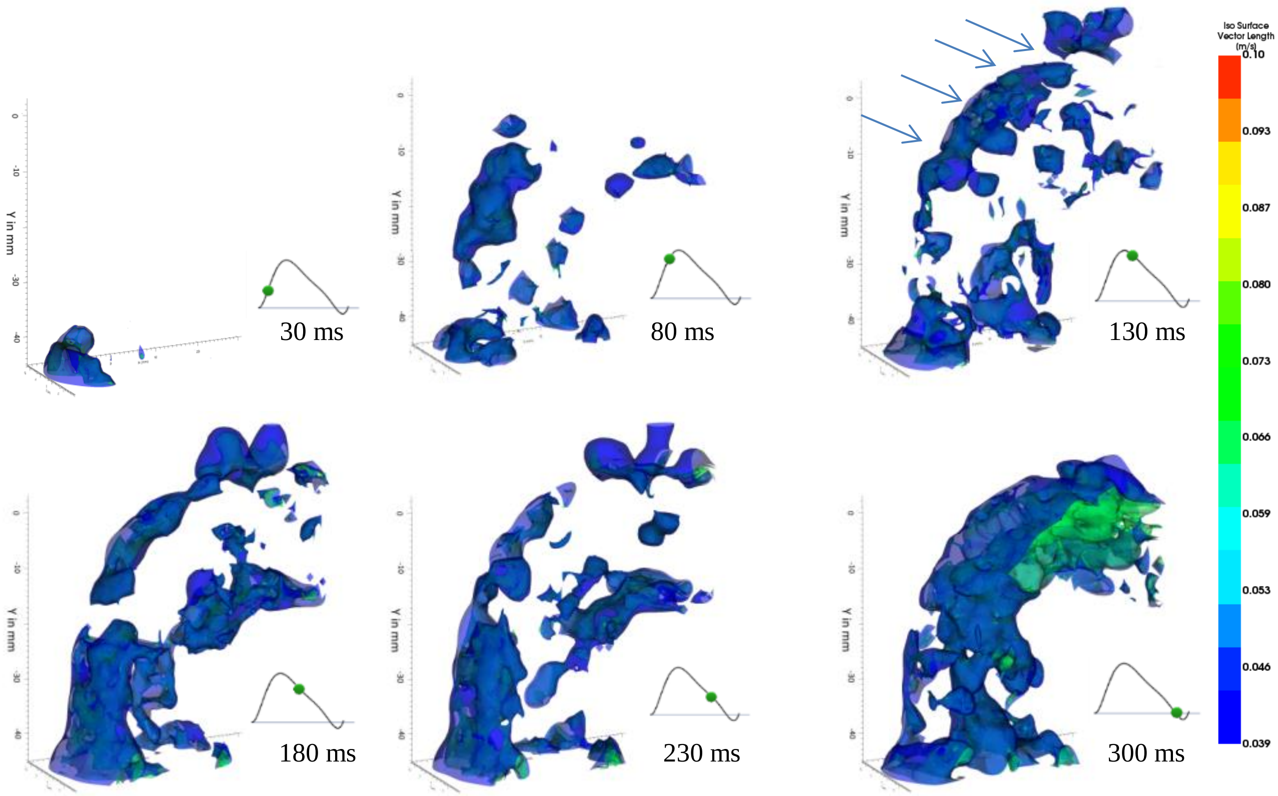

Fig. 6: Visualization of iso-surfaces for six different time steps referring to Fig. 5. Three iso-surface regions are shown, with velocities of 0.01 m/s (blue), 0.05 m/s (green) and 0.1 m/s (red). Shortly after the opening of the valve, the velocities in the whole arch range over 0.1 m/s, except in the right bulb. With growing time, low velocity regions are developing on the walls and in the inner regions of the aorta.

3.5 CONCLUSION AND OUTLOOK

The presented data analysis shows the flow through the aortic arch in a 3D volume to get a better understanding of the interaction of the heart valve, the flow and the inner walls. We used the 3D PTV method to determine the single particle trajectories over a long observation time and the theoretically residence time. The results were extended by 3D PIV measurements obtaining the global velocity field, which showed the complexity of the pulsating flow that was generated in the aortic arch. It was found that at the beginning of the heart valve a wash out flow over the complete 180° arch was generated and no flow separations occurred. During this acceleration phase an eccentrically located core flow in the ascending arch developed. The core flow first appeared toward the inner wall and moved with growing time around to the outer wall, due to the centrifugal force. Same results were presented by Kilner et al. [10]. They applied time resolved phase contrast magnetic resonance imaging (PC MRI) investigating the distribution of secondary flows in the aortic arch in

10 healthy humans. Our analyzed peak velocity of the ascending aortic arch of about 0.9 m/s is in the same order that Kilner et al.[10] measured with 0.96 m/s ± 0.06. They mentioned as well that helical and retrograde streams are consistent features of intra-aortic flow in healthy subjects that result partly from the curvature of the arch and the pulsatility of flow in it. Due to the simplified artic geometry, which is not torsional as found in humans, the development of the typical helical structure was not that explicit. The pulsatility of flow in the aortic arch led to retrograde movement along the inner curvature. Higher pressure, stronger washout and stronger mixing is expected compared to stationary flow, which leads to optimal blood transport through the aorta. The particles near the inner wall accelerated more readily in early systole and decelerated more readily in late systole, a migration of the highest velocities outward was observed in the arch, and a retrograde stream arises from relatively slow blood close to the inner curvature [10,11]. At the end of the heart cycle at 300 ms when the weight of the inertial effects led to a disorganization of the flow field the flow contained multiple, small-scale eddies and counter eddies whose distribution and movements were chaotic.
For a conclusive overview of the aortic arch measurements, it is planned to measure the wall shear stress distribution simultaneous to the 3D flow by using micro flap structures. This enables to ensure the values of the wall shear stress working on the blood cells near the outer wall regions and the endothelial cells. While large values of wall shear stresses increase the risk of atherosclerosis, thrombi are formed in places with constantly low wall shear stresses [12].

REFERENCES

[1] Vasava P, et al.(2009) Computational Study of Pulsatile Blood Flow in Aortic Arch: Effect of blood Pressure. (Eds.): WC 2009, IFMBE Proceedings 25/IV

[2] Brücker C, et al. (2002) Unsteady flow through a new mechanical heart valve prosthesis analysed by digital particle image velocimetry. Meas. Sci. Technol. 13:1043–1049

[3] Krempl T K (2002) Entwicklung eines künstlichen Herz-Kreislauf-Modells zur hämodynamischen Evaluation von Aortenklappenprothesen. urn:nbn:de:gbv:27-dbt-001534-6

[4] Lim W L, Chew Y T, Chew T C, Low H T (1998) Steady flow dynamics of prosthetic aortic heart valves: a comparative evaluation with PIV techniques. J Biomech 1998; 31(5):411-421

[5] Walker P G, Yoganathan A P (1992) In vitro pulsatile flow hemodynamics of five mechanical aortic heart valve prostheses. Eur J Cardiothorac Surg 1992; 6 Suppl 1:S113-S123

[6] Hegner F, Kamps L, Brücker C (2014) 3D Scanning Stereo PIV in heart valve flows. Conference: 17th Int. Symp. Appl. Laser Techniques to Fluid Mech, At Lisbon

[7] Sproul A, Simpson E (1964) Stroke Volume and related Hemodynamic Data in normal Children. Pediatrics Vol. 33 No. 6 June 1, pp. 912 - 918

[8] Atkinson C, Soria j (2009) An efficient simultaneous reconstruction technique for tomographic particle image velocimetry. Exp Fluids 47:553–568; DOI 10.1007/s00348-009-0728-0

[9] Westfeld P, Maas H G, Pust O, Kitzhofer J, Brücker C (2010) 3-D Least Squares Matching for Volumetric Velocimetry Data Processing" 15th Int Symp on Applications of Laser Techniques to Fluid Mechanics Lisbon, Portugal, 05-08 July, 2010

[10] Kilner P J, Yang G Z, Mohiaddin R H, Firmin D N, Longmore D B (1993) Helical and Retrograde Secondary Flow Patterns in the Aortic Arch Studied by Three-Directional Magnetic Resonance Velocity Mapping. Circulation, 88, part 11:2235-2247

[11] Morbiducci U, Ponzini R, Rizzo G, Cadioli M, Esposito A, De Cobelli F, Del Maschio A, Montevecchi F M , Redaelli A (2009) In Vivo Quantification of Helical Blood Flow in Human Aorta by Time-Resolved Three-Dimensional Cine Phase Contrast Magnetic Resonance Imaging. Annals of Biomedical Engineering. January 2009. DOI: 10.1007/s10439-008-9609-6

[12] Zürcher L (2003) Simulation der Strömung in der menschlichen Aorta. d-nb.info/100936393X/34